

分布式拉杆转子轴向预紧力的确定

张青雷,陈堰芳,程义悦

(上海理工大学 机械工程学院,上海 200093)

摘 要:研究了分布式拉杆转子在考虑轮盘间接触效应时轴向预紧力的确定方法。分析了拉杆转子在不同工况下的转子最大等效应力,轮盘结合面最大、最小法向接触应力及转子弯曲刚度随拉杆预紧量变化的规律。结果表明:随着转子轴向预紧力的增加,转子能够传递更大的载荷,其弯曲刚度、固有频率与连续体的偏差更小,但转子的最大等效应力显著增加,材料的强度裕度显著降低。根据得到的拉杆转子最大等效应力结果、接触面法向应力分布、转子弯曲刚度结果及转子自由模态频率结果,确定了转子合适的轴向预紧力。当转子承受 100 kN 的切向载荷时,转子合适的预紧量范围为拉杆总长的 7/10000—13/10000。

关 键 词: 拉杆转子; 轴向预紧力; 弯曲刚度; 有限元分析

中图分类号: TH133 文献标识码: A

引 言

拉杆转子通过拉杆将轮盘和轴头及鼓筒等结构预紧组合在一起,成为一种组合式转子,具有重量轻、冷却好、易装配等优点,在燃气轮机中得到广泛的应用^[1-2]。为了保证高速旋转的转子安全可靠地工作,装配时需要通过调整拉杆的预紧量来施加适当的轴向预紧力^[3-5]。文献[6]建立了一种新的确定转轴系统的理想轴向预紧力的理论模型,并且给出了转轴的形变与预紧力的变化关系。文献[7]提出了燃气轮机拉杆转子结构完整性概念,给出了转子在不同运行工况中应力的变化规律。文献[8]组装了一个简易的加载夹具,并对其进行了低振幅的调幅测试和高振幅的冲击载荷测试,分析了夹具在不同预紧力下的线性 and 非线性响应特点。文献[9]建立了螺栓连接转子结构有限元计算模型,计算了发动机各个功率下连接螺栓的压紧力/松弛力,确定了某涡扇发动机转子连接螺栓的轴向预紧力。文献[10-11]提出了综合考虑拉杆紧度裕度、强度裕度、装配关系等多种因素的轴向预紧力确定准则,通过对中心拉杆凸肩与其接触零件在工作中是否出现

分离现象的研究,为解决端齿连接转子轴向预紧力的确定问题提供了实用方法。文献[12]对周向均布拉杆转子进行有限元应力分析,得到了不同预紧力和运行工况下转子的应力分布及界面接触状态演化规律,给出了保证转子结构完整性和结构强度要求的预紧力确定方法。

合适的转子轴向预紧力要保证转子结构完整性和结构强度要求,还要保证转子在弯曲、扭转刚度等性能参数上与连续转子接近,并要经过动力学特性分析来验证转子的综合性能能达到要求。本研究以分布式拉杆转子为研究对象,进行不同拉杆预紧力和工况下转子的结构静力分析,在保证转子结构完整性的前提下,保持转子具备足够的安全裕度,保证转子在弯曲刚度性能参数上与连续转子接近,从而确定转子轴向预紧力,通过不同拉杆预紧量下转子的自由模态分析,对确定的转子轴向预紧力进行了验证。

1 模态分析理论基础

在工程实际振动问题中,经常应用有限单元法对结构进行动力学特性分析。对于一个 N 自由度机械系统,其运动方程可表示为^[13]:

$$[M]\{\ddot{u}\} + [C]\{\dot{u}\} + [K]\{u\} = \{F(t)\} \quad (1)$$

式中: $[M]$ 、 $[C]$ 、 $[K]$ —系统的质量矩阵、阻尼矩阵、刚度矩阵; $\{F(t)\}$ —激励载荷向量; \ddot{u} 、 \dot{u} 和 u —系统的加速度向量、速度向量和位移响应向量。

式(1)为一个耦合的多维方程组,左右两边同时进行拉氏变换,令 $s = j\omega$, 可得:

$$\{[K] - \omega^2[M] + j\omega[C]\}\{X(\omega)\} = \{F(\omega)\} \quad (2)$$

将式(2)引入模态坐标解耦。令 $\{X\} = [\varphi]\{q\}$, 得:

收稿日期: 2014 - 06 - 03; 修订日期: 2014 - 06 - 13

作者简介: 张青雷(1973 -),男,上海人,博士,上海理工大学研究生导师,教授级高级工程师。

$$\{ [K] - \omega^2 [M] + j\omega [C] \} [\varphi] \{q\} = F \quad (3)$$

式中: $[\varphi]$ —系统各阶振型对应的振型矩阵;
 $\{q\}$ —模态坐标。

对式(3)进行正交化处理,使其成为在模态坐标系统中相互独立的 N 自由度系统的方程组,则将其解耦后第 i 个独立的方程为:

$$\{ K_i - \omega^2 M_i + j\omega C_i \} q_i = \sum_{j=1}^n \varphi_{ji} F \quad (j = 1, 2, \dots, n) \quad (4)$$

在模态坐标系统中,质量 M_i 、刚度 K_i 、阻尼 C_i 和固有振型 φ_i 均称为系统的模态参数,分别称为模态质量、模态刚度、模态阻尼及模态振型。采用模态归一化的方法将模态质量、模态刚度归一,设模态质量、刚度归一化振型为 $[\Phi]$ [14],得:

$$[\Phi]^T [M] [\Phi] = [I] \quad (5)$$

$$[\Phi]^T [K] [\Phi] = [\omega_i^2] \quad (6)$$

其中, $\omega_i = \sqrt{K_i/M_i}$ 为系统固有频率。

2 不同预紧量下拉杆转子静力分析

2.1 分布式拉杆转子计算模型

分布式拉杆转子如图 1 所示,由 8 根均布的拉杆将四级轮盘及两端轴头预紧成一个整体。针对轮盘结合面间接触行为的复杂性,依据转子结构特点,采用周向均布弹簧单元模拟轮盘间的接触效应,不考虑接触摩擦。

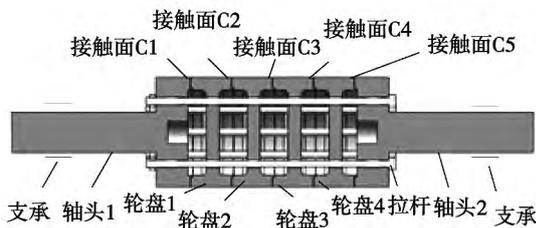


图 1 转子示意图

Fig. 1 Schematic diagram of the rotor

为保证应力计算的精度,需要对转子进行合理的网格划分。网格数目增加到一定程度,网格质量越高,网格越密集,应力计算精度就越高。将转子实体模型导入 Hypermesh 软件中进行网格划分,得到全局均匀细化的六面体网格模型如图 2 所示,共包括 135160 个单元,163861 个节点。将网格导入 ANSYS 软件中进行计算。

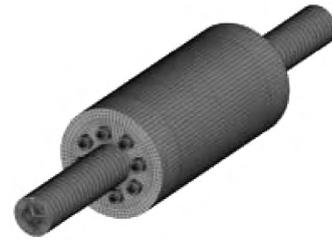


图 2 转子网格模型

Fig. 2 Model for the grid of the rotor

轴向预紧力与预紧量的关系可表示为:

$$\Delta l = FL / (EA) \quad (7)$$

式中: Δl —预紧量, m ; F —轴向预紧力, N ; L —拉杆有效长度, m ; E —拉杆材料弹性模量, Pa ; A —拉杆有效截面积, m^2 。根据式(7),可以将轴向预紧力转化为预紧量。

2.2 转子应力分析

拉杆转子的最大轴向预紧力要保证转子工作时各零部件不损坏。根据转子的最大等效应力计算结果,结合材料的许可屈服极限,可以确定最大轴向预紧力。

在图 1 所示的轮盘 3 上施加切向载荷,将转子两端支承处固定,对转子进行结构静力分析,不考虑离心力的影响。查看转子的最大等效应力随预紧量和切向载荷的变化情况,计算结果如表 1 所示。在拉杆预紧量为拉杆总长 9/10000 和切向载荷为 100 kN 共同作用下,转子的等效应力分布如图 3 所示。

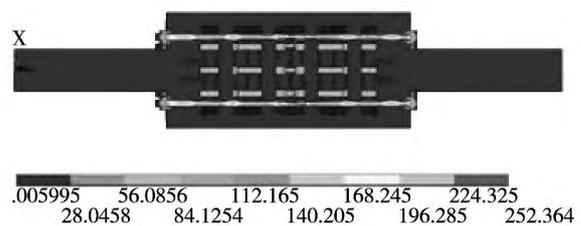


图 3 转子的等效应力分布 (MPa)

Fig. 3 Equivalent stress distribution of the rotor

从图 3 可知,拉杆转子的最大等效应力出现在拉杆上,轮盘和转轴上的等效应力较小。由表 1 可知,转子的最大等效应力随着预紧量和切向载荷的变化趋势符合转子静力学理论。查材料手册,转子材料的许用应力为 375 MPa。以拉杆转子承受 100 kN 切向载荷为例,在为拉杆总长 13/10000 的预紧量作用下,转子的最大等效应力约为 364 MPa,继续

增加预紧量后转子的最大等效应力大于许用应力, 不符合要求。因此 将为拉杆总长 13/10000 的预紧量作为此时拉杆转子的最大预紧量。

表 1 转子的最大等效应力 (MPa)

Tab. 1 Maximum equivalent stress of the rotor (MPa)

切向载 荷/kN	预紧量与拉杆总长的比值(1/10000)					
	5	7	9	11	13	15
0	139.743	195.641	251.538	307.436	363.333	419.237
25	139.925	195.796	251.692	307.591	363.475	419.364
50	140.119	195.937	251.837	307.738	363.639	419.541
75	140.436	196.325	252.103	307.924	363.792	419.697
100	140.881	196.616	252.364	308.113	363.924	419.824
125	141.524	196.973	252.721	308.463	364.241	420.112
150	141.889	197.396	253.116	308.861	364.614	420.358
175	142.653	197.742	253.502	309.287	364.923	420.769
200	143.142	198.409	253.918	309.623	365.362	421.107
225	143.961	198.916	254.471	310.135	365.753	421.437
250	144.586	199.631	254.939	310.439	366.129	421.861
275	145.217	200.254	255.528	310.872	366.547	422.278
300	146.106	200.966	256.133	311.461	366.965	422.643

2.3 轮盘接触面法向接触应力分析

查看转子 5 个接触面 C1、C2、C3、C4 和 C5 的法向接触应力在预紧量为拉杆总长 9/10000 作用下的变化情况, 如图 4、图 5 所示。

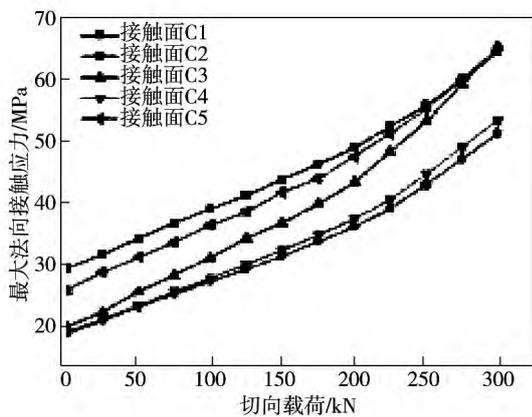


图 4 各接触面最大法向接触应力
Fig. 4 Maximum normal contact stress on various contact surfaces

由图 4、图 5 可知, 接触面 C1 的法向接触应力随切向载荷的变化最小。接触面 C3、C4 在切向载荷增大时最小法向接触应力下降很快, 而且 C3 最

小接触应力最先下降为零, 最易发生局部分离; 在相同载荷情况下, C3 处最大法向接触应力比 C4 大, 随着切向载荷的增大, C3 最大法向接触应力的增长速度比 C4 要快, 表明在 C3 处最容易出现局部挤压。这说明在确定轴向预紧力时应重点保证 C3 保持不分离。图 6 为在拉杆预紧量为拉杆总长 9/10000 和切向载荷为 100 kN 共同作用下, 接触面 C3 的法向接触应力分布。图 7、图 8 分别为转子在不同预紧量下危险接触面 C3 承受不同切向载荷时的最大、最小法向接触应力。其中, l/L 表示预紧量与拉杆总长的比值。

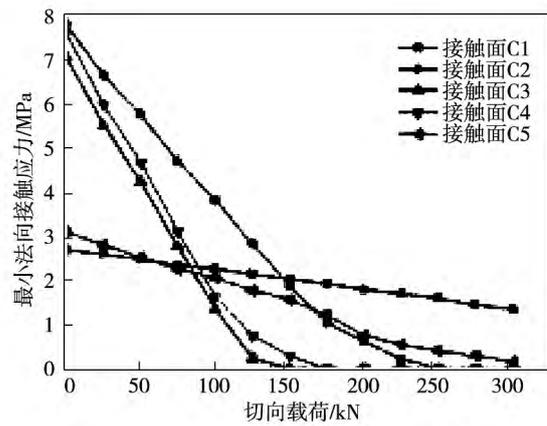


图 5 各接触面最小法向接触应力
Fig. 5 Minimum normal contact stress on various contact surfaces

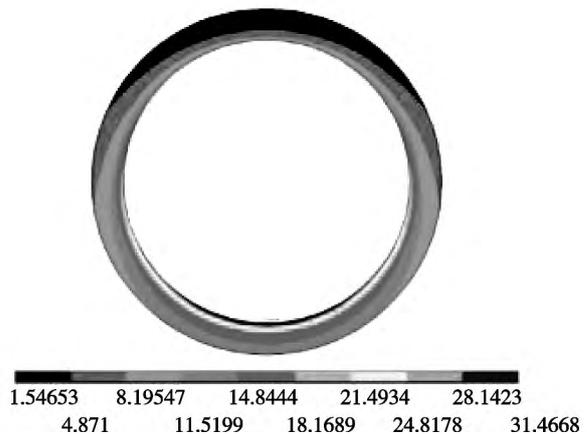


图 6 接触面 C3 的法向接触应力分布 (MPa)
Fig. 6 Distribution of the normal contact stress on the contact surface C3

由图 6 可知, 接触面 C3 出现局部挤压, 最大法向接触应力出现在接触面挤压部分的内圈, 最小法

向接触应力出现在接触面挤压部分的外圈。这是因为位于接触面内圈的拉杆预紧时,轮盘 2 首先与轮盘 3 的内侧接触,轮盘 3 内侧发生变形,轮盘 2 才会与轮盘 3 外侧接触。由图 7、图 8 可知,接触面 C3 的最大最小法向接触应力随预紧量和切向载荷的变化符合转子静力学理论。

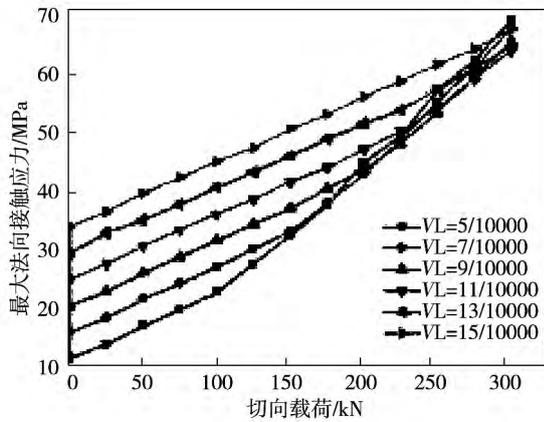


图 7 接触面 C3 最大法向接触应力 (MPa)

Fig. 7 Maximum normal contact stress on the contact surface C3 (MPa)

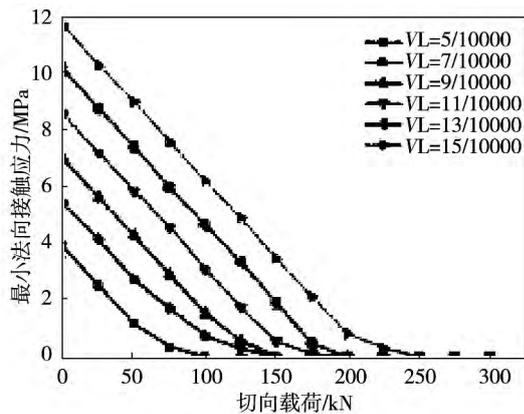


图 8 接触面 C3 最小法向接触应力 (MPa)

Fig. 8 Minimum normal contact stress on the contact surface C3 (MPa)

拉杆转子最小轴向预紧力要保证转子工作时轮盘接触面不分离,从而保证转子的结构完整性。根据轮盘接触面法向接触应力分析中得到的接触面最小法向接触应力判断接触面是否发生分离,可以确定最小轴向预紧力。当转子承受 100 kN 切向载荷时,在为拉杆总长的 5/10000 的预紧量作用下最小法向接触应力为零,局部发生了分离,应增加预紧

量。增加预紧量到拉杆总长的 7/10000 时,最小法向接触应力大于零,未发生局部分离,可考虑以此作为此时拉杆转子的最小预紧量。

2.4 分布式拉杆转子弯曲刚度分析

根据应变能理论^[15]计算得到不同预紧量下转子接触段的弯曲刚度,并与连续转子的弯曲刚度进行对比。计算结果如表 2 所示。

表 2 转子弯曲刚度

Tab. 2 Bending stiffness of the rotor

预紧量/拉杆总长	弯曲刚度(10 ⁻⁸ N/m)	偏差/%
5/10000	1.57301	11.76398
7/10000	1.62320	8.94863
9/10000	1.65580	7.11998
11/10000	1.67796	5.87694
13/10000	1.69305	5.03049
15/10000	1.70631	4.28668
连续转子	1.78273	

由表 2 可知:当预紧量为拉杆总长的 7/10000—13/10000 时,拉杆转子与连续转子弯曲刚度的偏差小于 10%,表明在该预紧力作用下,拉杆转子的弯曲刚度接近同形状连续转子。以连续转子作为参照,此预紧力下拉杆转子的整体弯曲刚度性能参数符合要求。

3 转子模态分析

对转子进行自由模态分析,作为比较,同时对连续转子进行自由模态分析,提取前 3 阶固有频率的计算结果列于表 3,预紧量为拉杆总长的 9/10000 时作用下转子的前 3 阶弯曲振型如图 9 所示。

由表 3 和图 9 可知,预紧量的变化对转子第 1、2 阶固有频率影响不大,但是对第 3 阶的影响较为明显。当预紧量为拉杆总长的 7/10000—13/10000 时,拉杆转子的弯曲固有频率与连续转子十分接近,模态振型也一致,并且振幅大小也十分接近。

根据以上模态分析,可知预紧量为拉杆总长的 7/10000—13/10000 时,拉杆转子能够很好地保持其模态的完整性。这表明了为拉杆总长 7/10000—13/10000 的预紧量是合适的。同时,证明了本研究拉杆转子轴向预紧力的确定方法是有效的。

表 3 转子前 3 阶固有频率

Tab.3 First three - order intrinsic frequencies of the rotor

预紧量/拉杆总长	第 1 阶	第 2 阶	第 3 阶
5/10000	340.16	460.43	1302.4
7/10000	340.86	460.73	1316.5
9/10000	341.30	460.92	1325.4
11/10000	341.58	461.04	1331.3
13/10000	341.79	461.13	1335.6
15/10000	341.94	461.19	1338.9
连续转子	342.51	461.43	1350.9



图 9 转子弯曲振型

Fig.9 Bending vibration modes of the rotor

4 结 论

对分布式拉杆转子进行考虑轮盘间接触效应的有限元结构静力分析,给出了不同预紧量和工况下转子最大应力、轮盘结合面最大、最小法向接触应力及转子弯曲刚度的变化情况。结果表明:

(1) 增加转子轴向预紧力,转子能够传递更大的载荷,其弯曲刚度与连续体的偏差更小,更能体现拉杆转子的优点,其固有频率与连续体的偏差也 smaller,更能保持模态的完整性,但转子的最大等效应力显著增加,材料的强度裕度显著降低。

(2) 以拉杆转子承受 100 kN 的切向载荷为例,根据转子的最大等效应力确定的最大预紧量为拉杆总长的 13/10000,根据对轮盘接触面法向接触应力确定的最小预紧量为拉杆总长的 7/10000,转子的模态分析表明,当预紧量为拉杆总长的 7/10000 -

13/10000 时,拉杆转子的弯曲固有频率与连续转子十分接近,模态振型一致,振幅大小也十分接近。通过转子模态分析结果的验证,表明了本研究所确定的轴向预紧力是合适的,转子轴向预紧力的确定方法是有效的,为同类转子轴向预紧力的确定提供了参考依据。

参考文献:

[1] ZHANG Yan-chun ,DU Zhao-gang ,SHI Li-ming ,et al. Determination of contact stiffness of rod-fastened rotors based on modal test and finite element analysis [J]. Journal of Engineering for Gas Turbine and Power 2010 ,132(9) : 945.

[2] YUAN Qi ,GAO Jin ,LI Pu. Nonlinear dynamics of the rod-fastened Jeffcott rotor [J]. Journal of Vibration and Acoustics ,2014 ,136(2) : 210 - 220.

[3] Michael D. Wolfe. Ultrasonic bolt load measurement [J]. Diesel and Gas Turbine Worldwide ,2005 ,37(8) : 84 - 88.

[4] LU Ming-jian ,GENG Hai-peng ,YANG Bai-song ,et. al. Finite element method for disc-rotor dynamic characteristics analysis of gas turbine rotor considering contact effects and rod preload [C]. Xi'an: Mechatronics and Automation(ICMA) 2010 ,1179 - 1183.

[5] 郭飞跃 ,邓旺群 ,成晓鸣. 涡轴发动机组合压气机转子轴向预紧力计算方法[J]. 航空动力学报 ,2004 ,19(5) : 623 - 629.

GUO Fei-yue ,DENG Wang-qun ,CHENG Xiao-ming. A method for calculating the axial pretightening force of the combined compressor rotor of a turbo-shaft engine [J]. Journal of Aerospace Power , 2004 ,19(5) : 623 - 629.

[6] SHAN Xiao-biao ,Xie Tao ,Chen Wei-shan. Novel approach for determining the optimal axial preload of a simulating rotary table spindle system [J]. Journal of Zhejiang University. Science A , 2007 ,8(5) : 812 - 817.

[7] Janssen M J ,Joyce J S. 35-year old splined-disc rotor design for large gas turbine [EB/OL]. [2009 - 03 - 19]. <http://www.electricity-today.com/et/Oct96/turb.htm>.

[8] Charles Matthew Butner ,Douglas E. Adams ,Jason R. Foley. Experimental investigation of the effects of bolt preload on the dynamic response of a bolted interface [J]. J. Appl. Mech ,2013 ,80(1) : 1 - 14.

[9] 刘 存. 航空发动机转子连接螺栓预紧力与疲劳寿命研究 [D]. 南京: 南京航空航天大学 ,2009.

LIU Cun. Research of the pretightening force and fatigue life of the connecting bolts in an aero-engine rotor [D]. Nanjing University of Aeronautics and Astronautics 2009.

[10] 尹泽勇 ,胡柏安 ,吴建国 ,等. 端齿连接转子轴向预紧力的确定 [J]. 航空动力学报 ,1996 ,11(4) : 355 - 357.

YIN Ze-yong ,HU Bai-an ,WU Jian-guo ,et al. Determination of the axial pretightening force of the end teeth connecting a rotor [J]. Journal of Aerospace Power ,1996 ,9(2) : 355 - 357.

[11] 胡柏安 ,尹泽勇 ,徐友良. 两段预紧的端齿连接转子轴向预紧

力的确定[J]. 机械强度, 1999, 21(4): 274 - 277.

HU Bai-an, YIN Ze-yong, XU You-liang. Determination of the axial pretightening force of the end teeth connecting a rotor pretightened in two sections[J]. Mechanical Strength, 1999, 21(4): 274 - 277.

[12] 李辉光, 刘恒, 虞烈. 周向均布拉杆转子预紧力的确定[J]. 航空动力学报, 2011, 26(12): 2791 - 2797.

LI Hui-guang, LIU Heng, YU Lie. Determination of the pretightening force of a tie-rod rotor uniformly distributed in the circumferential direction [J]. Journal of Aerospace Power, 2011, 26(12): 2791 - 2797.

[13] 于天彪, 王学智, 关鹏, 等. 超高速磨削机床主轴系统模态分析[J]. 机械工程学报, 2012, 48(17): 183 - 188.

YU Tian-biao, WANG Xue-zhi, GUAN Peng, et al. Modal analysis of the spindle system of an ultra-high speed grinder [J]. Journal of Mechanical Engineering, 2012, 48(17): 183 - 188.

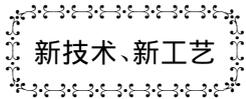
[14] 林贤坤, 覃柏英, 张令弥, 等. 基于附加质量的实验模态振型质量归一化[J]. 振动、测试与诊断, 2012, 32(5): 784 - 790.

LIN Xian-kun, QIN Bai-ying, ZHANG Ling-mi, et al. Mass normalization of the test modal vibration mode based on an addition of mass [J]. Journal of Vibration, Measurement & Diagnosis, 2012, 32(5): 784 - 790.

[15] 李浦, 袁奇, 高进, 等. 轮盘端面齿连接的周向拉杆转子刚度研究[J]. 2013, 28(7): 1618 - 1623.

LI Pu, YUAN Qi, GAO Jin, et al. Investigation of the stiffness of a circumferential tie-rod rotor connected by the end surface teeth of a wheel disk [J]. Journal of Aerospace Power, 2013, 28(7): 1618 - 1623.

(丛敏 编辑)



495 MW 格兰德里弗 M501J 联合循环发电项目

据《Gas Turbine World》2013年11-12月刊报道,格兰德里弗大坝管理局,俄克拉荷马州国营电力事业公司,已与三菱重工动力系统(美国)签订合同,供货一台M501J燃气轮机用于舒蒂奥电站工程。

J系列燃气轮机是正在塔尔萨以东约56 km舒蒂奥建造的495 MW燃气轮机联合循环发电系统的核心设备。

供给格兰德里弗大坝管理局的联合循环电站成套设备包括:1台M501J燃气轮机、1台SRT-50汽轮机和1台发电机。燃气轮机将由佐治亚州萨瓦纳市萨瓦纳机器厂制造,该厂是三菱重工在美国的制造基地。发电机将由三菱电气公司供货。

三菱重工声称,该燃机2011年面市以来,公司已经收到28台M501J燃气轮机订单。目前正在使用的9台J系列燃气轮机总运行时间已超过28 000 h。

舒蒂奥电站联合循环装置计划于2017年投入运行。借助于对燃煤发电的依赖性,该装置将有助于格兰德里弗大坝管理局满足新的排放要求。

MHI研制的M501J燃气轮机及其联合循环装置是当今世界上热效率最高的大功率发电装置。在ISO条件下,M501J燃机在基本负荷上的额定输出功率为327 MW,热效率为41.0%;M501J燃机的MPCPI联合循环装置的净输出功率为470 MW,热效率为61.5%。

(吉桂明 摘译)

frequency modulation on the dynamic thermal characteristics of the supercritical steam turbine was studied. By using a method combining the lumped parameters with distribution parameters a dynamic mathematical model was established for the units and the static and dynamic characteristics of the units under various operating conditions was analyzed with the law governing the influence of the load disturbance and parameters of the control system under different operating conditions on the flow rate of the units, pressure and temperature after the regulating stage and temperature after the reheater being obtained. It has been found that with an increase of the load disturbance, whatever the units are in constant pressure and sliding pressure operation, the percentage overshoots of various physical quantities during the dynamic process are constant and changes of the temperatures in various HP, IP and LP stages of the units can be neglected. When the units are in sliding pressure operation, under the condition of the temperature at the outlet of the boiler being kept constant, with an increase of the time constant in both flow rate-pressure link and power-flow rate link, any change in the temperature after the HP regulating stage is approximately 1.5 °C and that after the reheater is about 0.2 °C. Therefore, the influence of the primary frequency modulation on the dynamic characteristics of the thermal parameters in the supercritical units under various operating conditions is very small and will not affect the safety and stability of the units in operation. **Key Words:** primary frequency modulation, supercritical unit, constant pressure operation, sliding pressure operation, dynamic thermal characteristics

分布式拉杆转子轴向预紧力的确定 = **Determination of the Axial Pretightening Force of a Distributed Type Tie-rod Rotor** [刊, 汉] ZHANG Qing-lei, CHEN Yan-fang, CHENG Yi-yue (College of Mechanical Engineering, Shanghai University of Science and Technology, Shanghai, China, Post Code: 200093) // Journal of Engineering for Thermal Energy & Power. -2014, 29(5). -477-482

Studied was the method for determining the axial pretightening force of a distributed type tie-rod rotor when the contact effect between the wheel disks being taken into account and analyzed was the variation law governing the maximal equivalent stress of the rotor, maximal and minimal normal contact stress on the joint surfaces of the wheel disks and the bending rigidity of the rotor under various operating conditions with the pretightening amount of the tie-rod. It has been found that with an increase of the axial pretightening force of the rotor, the rotor can transfer a growing load and the deviation between its bending rigidity and intrinsic frequency and those of its continuum will become smaller, however, the maximal equivalent stress of the rotor will remarkably increase and the strength allowance of the material will markedly decrease. On the basis of the maximal equivalent stress of the tie-rod rotor, normal stress distribution on the contact surface, the bending rigidity and the free mode frequency of the rotor obtained, a proper axial pretightening force of the rotor was determined. When the rotor sustains a shear load of 100 KN, the proper pretightening force range of the rotor will be 7/10000 to 13/10000 of the total length of the tie-rod rotor. **Key**

Words: tie-rod rotor ,axial pretightening force ,bending rigidity ,finite element analysis

低压汽轮机末级长叶片改型试验研究 = **Experimental Study of a Retrofitted Long Blade Used in the Last Stage of a LP Steam Turbine** [刊 ,汉] KANG Lei ,YU Jian-feng ,WANG Chao (CSIC No. 703 Research Institute , Harbin ,China ,Post Code: 150078) ,LIANG Yao (China Electric Power Engineering Co. Ltd. ,Beijing ,China ,Post Code: 100048) //Journal of Engineering for Thermal Energy & Power. -2014 29(5) . -483 -491

In the light of such operation characteristics of marine steam turbines as off-design operating conditions and a big wetness in several stages before the last one ,dynamically optimized was the long blades in the last stage of a steam turbine and air-blowing tests were performed of the prototype and retrofitted totaling two cascades on an annular cascade test rig at three mach numbers at the outlet and at five attack angles. It has been found that with an increase of the Mach number after the cascades ,the location of the lowest pressure point on the suction surface of the blades will shift rearwards ,the pressure dropping section in the front half section of the cascades will become longer ,the pressure gradient along the pressure dropping direction increase ,the boundary layer become thinner and the blade profile loss decrease. The secondary flow loss on the outside end wall of the rotating blades after the retrofiting will markedly drop and enhance the applicability to attack angles. The positive and negative attack angles will only affect the static pressure distribution on the suction surface or pressure surface at the leading edge of the blades. At any Mach number ,any increase in the absolute attack angle will all lead to an increase of the loss in the cascades. **Key Words:** off-design operating condition ,long blade ,twisted blade ,wind tunnel test ,total pressure loss coefficient

燃气轮机拉杆转子的轮盘结合面接触模型研究 = **Study of the Contact Model for Joint Surfaces of Wheel Disks on Tie-rod Rotors in Gas Turbines** [刊 ,汉] ZHANG Qing-lei ,CHEN Yan-fang ,ZHAO Bai-yu (College of Mechanical Engineering ,Shanghai University of Science and Technology ,Shanghai ,China ,Post Code: 200093) // Journal of Engineering for Thermal Energy & Power. -2014 29(5) . -492 -497

To establish a more accurate finite element model for tie-rod rotors of gas turbines ,studied were the mechanic contact models for joint surfaces of wheel disks of tie-rod rotors. By using a spring unit to simulate the contact on the joint surfaces of the wheel disks ,the contact models were improved based on the joint surfaces and the fitting curves showing the relationship between the normal contact rigidity on the joint surfaces and the pretightening force were obtained. It has been found that with an increase of the load normal to the joint surfaces ,the contact rigidity will become bigger ,however ,after the normal load exceeds a certain value ,if keeping on increasing ,the increasing tendency of the contact rigidity will become slower. According to the fitting curves ,the contact rigidity value corresponding